



Cite this: *Phys. Chem. Chem. Phys.*,
2019, 21, 8883

Fluorescence measurements of peroxyxynitrite/ peroxyxynitrous acid in cold air plasma treated aqueous solutions

Barbora Tarabová,^{id}*^a Petr Lukeš,^{id}^b Malte U. Hammer,^{†c}
Helena Jablonowski,^{id}^c Thomas von Woedtke,^{id}^d Stephan Reuter^{id}^{†c} and
Zdenko Machala^{id}^a

Qualitative detection of peroxyxynitrite/peroxyxynitrous acid (ONOO⁻/ONOOH) as one of the key bactericidal agents produced in cold air plasma activated aqueous solutions is presented. We examined the use of the 2,7-dichlorodihydrofluorescein diacetate (H₂DCFDA) fluorescent dye to detect ONOO⁻/ONOOH in plasma activated non-buffered water (PAW) or buffered solution (PAPB) generated by DC-driven self-pulsed transient spark discharge at atmospheric pressure in ambient air. The diagnostic selectivity of H₂DCFDA to reactive oxygen and nitrogen species (RONS) typical of plasma activated aqueous solutions was examined by using various scavengers of RONS. This cross-reactivity study showed the highest sensitivity of the H₂DCFDA dye to ONOO⁻/ONOOH. However, besides ONOO⁻/ONOOH, H₂DCFDA also exhibited sensitivity to hypochlorite anions/hypochlorous acid (OCl⁻/HOCl), showing that for a selective study it is important to have an idea about the possible constituents in the studied solutions. The sensitivity of H₂DCFDA to other RONS even in much higher concentrations was negligible. The presence of nitrites (NO₂⁻) and hydrogen peroxide (H₂O₂) in PAW led predominantly to the production of peroxyxynitrous acid with a strong fluorescence response of H₂DCFDA in PAW. Plasma treatment of buffered solutions led to the weak response of H₂DCFDA. The fluorescence induced in PAW decreased after scavenging individual reactants, namely NO₂⁻ and H₂O₂, as well as by scavenging the product of the peroxyxynitrite forming reaction, proving that the fluorescence response of H₂DCFDA is primarily due to the formation of ONOO⁻/ONOOH. A chemical kinetics analysis of post-discharge processes and the pseudo-second order reaction between H₂O₂ and NO₂⁻ confirms formation of peroxyxynitrous acid in PAW with a rate in the order of tens of nM per second. The post-discharge evolution of the ONOOH formation rate was clearly correlated with the parallel detection of ONOO⁻/ONOOH by fluorescence spectroscopy using the H₂DCFDA dye.

Received 13th February 2019,
Accepted 1st April 2019

DOI: 10.1039/c9cp00871c

rsc.li/pccp

1. Introduction

Peroxyxynitrites *i.e.* the peroxyxynitrite anion (ONOO⁻) and peroxyxynitrous acid (ONOOH) are reactive nitrogen species of biological relevance that are known to be formed *in vivo*. The very fast reaction ($\sim 10^9$ – 10^{10} M⁻¹ s⁻¹)^{1–3} of free superoxide O₂^{•-} and nitric oxide •NO radicals, if present simultaneously

in vivo, results in the formation of peroxyxynitrite anions (eqn (1)).



ONOO⁻ exists in equilibrium with its conjugated acidic form – peroxyxynitrous acid ONOOH (pK_a 6.8) – (eqn (2)) and both species are present under typical biological conditions (~80% of ONOO⁻ at pH 7.4).



Both peroxyxynitrite forms are powerful oxidants that can oxidize cellular components directly or act as a nitrating agent. Furthermore, they can diffuse through cell membranes⁴ and mediate cytotoxic effects intracellularly. Thanks to their character they are suggested to be responsible for peroxyxynitrite-mediated pathological processes, *i.e.* ischemia/reperfusion

^a Faculty of Mathematics, Physics and Informatics, Comenius University, Mlynská dolina, 84248 Bratislava, Slovakia. E-mail: tarabova.barbora@gmail.com

^b Institute of Plasma Physics of the CAS, v.v.i., Za Slovankou 3, 18200 Prague, Czech Republic

^c Centre for Innovation Competence (ZIK) plasmatis, at INP Greifswald e.V., Felix-Hausdorff-Str. 2, 174 89 Greifswald, Germany

^d Leibniz Institute for Plasma Science and Technology (INP Greifswald e.V.), Felix-Hausdorff-Str. 2, 17489 Greifswald, Germany

[†] At the time of the studies.

injury, neurodegenerative diseases, cardiovascular disorders, atherosclerosis and severe inflammation conditions.^{2,5–8} Owing to this fact, peroxyxynitrite chemistry has been excessively investigated in biology and biochemistry with the focus on physiological conditions. Herein we present the peroxyxynitrite chemistry induced by cold plasma in liquids which involves processes at both acidic and neutral pH, with respect to its biological importance and bactericidal effects.

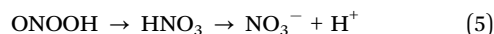
In recent years, cold (low-temperature) atmospheric pressure plasma treatment of bacteria, cells and tissues with or without contact with liquids has been shown to induce important biological effects, *e.g.* antimicrobial, therapeutic or apoptotic effects,^{9–11} which lead to various interesting bio-medical applications,¹² *e.g.* non-thermal decontamination/sterilization of liquids, heat sensitive materials or living tissues,^{13–15} applications in dentistry,^{16–18} wound healing,^{19–21} treatment of infective skin diseases or cancer treatment.^{22–24} Moreover, different studies demonstrated that aqueous solutions or media treated by cold plasmas, known as plasma activated water/media (PAW/PAM), possess significant antimicrobial^{25–28} or therapeutic properties.^{29–31} These effects can be attributed to formation of reactive oxygen and nitrogen species (RONS), and chemical changes induced by cold plasma treatment due to plasma-chemical reactions at the gas-liquid interface.^{32–34} Antimicrobial properties in air plasma activated non-buffered aqueous solutions are mainly attributed to the synergistic effects of the produced hydrogen peroxide H₂O₂ and nitrites NO₂[−] and the acidified pH.^{25,26,35–39}

Plasmas generated in ambient air or in gases with an admixture of N₂ and O₂ in direct contact with liquids generate gaseous RONS (*e.g.* nitrogen oxides NO_x, •OH and •OOH radicals, H₂O₂, HNO₂, HNO₃, O₃, *etc.*) which can penetrate or dissolve into the liquid and initiate chemical processes generating aqueous RONS. The most dominant aqueous species in PAW are long-lived species, such as H₂O₂, NO₂[−] and NO₃[−], or transient species like ONOO[−]/ONOOH, O₂•[−]/•OOH, •OH, •NO and •NO₂ radicals. Nitrites (NO₂[−]) and nitrates (NO₃[−]) in PAW are typically formed *via* the dissolution of gaseous nitrogen oxides NO_x (•NO and •NO₂), which is linked with the production of H⁺ (H₃O⁺) ions. This NO_x solvation, therefore, results in acidification of non-buffered plasma activated solutions. H₂O₂ is predominantly formed in the gas phase,^{40,41} as well as in PAW through the recombination of •OH radicals produced by plasma at the gas-liquid interface or *via* HO₂•/O₂•[−].⁴² The acidic conditions of PAW and the presence of NO₂[−] and H₂O₂ initiate the peroxyxynitrite chemistry and formation of the ONOO[−]/ONOOH couple during the plasma treatment, as well as during the post-discharge period *via* the reaction (eqn (3)):



Besides that, formation of ONOO[−] from •NO and O₂•[−] at neutral or alkaline pH is possible in buffered solutions (eqn (1)). Since some plasma sources emit significant UV emission, the possible formation of ONOO[−] due to UV photolysis of aqueous nitrites should not be neglected.⁴³ In addition, ONOO[−]/ONOOH might be also formed during plasma treatment

in the gas phase, for instance by the reaction of gaseous H₂O₂ with HNO₂ or the reaction of •OOH with •NO, subsequently followed by their fast dissolution due to the extremely high Henry's law solubility coefficient.⁴⁴ The actual form, the life-time and the reactivity of ONOO[−]/ONOOH are strongly pH-dependent. ONOOH present mainly in acidified PAW can in addition act indirectly through its acidic decomposition products – •OH and •NO₂ radicals (eqn (4)).^{6,39,45–47}



Although only ~30% of ONOOH decays into •OH and •NO₂ radicals (the rest dissociates into NO₃[−] *via* HNO₃ (eqn (5))),^{39,48} •OH and •NO₂ radicals induce strong cytotoxic effects and together with the acidic pH are assumed to be responsible for the strong bactericidal effect which has been described in multiple publications. Peroxyxynitrites even play a key role in the post-discharge bactericidal effect of PAW.^{26,38,39,49–51} Additionally, ONOOH participates in the formation of peroxyxynitric acid (O₂NOOH) by the reaction with H₂O₂, which can also contribute to the bactericidal properties of PAW.²⁷

The detection of peroxyxynitrites in general is difficult because of their high reactivity, very short life-time ranging from milliseconds to seconds, spontaneous decay, and typically very low concentrations (~nM) in biological systems. Likewise, the same problems arise in plasma activated liquids. Despite the present literature highlighting the importance of peroxyxynitrite chemistry for the antimicrobial properties of PAW, up to now only a few papers have demonstrated evidence of either the directly or indirectly measured presence of ONOO[−]/ONOOH in plasma activated liquids. Most of the techniques for assaying peroxyxynitrites use indirect methods relying on measurements of secondary species. Indirect biochemical assays are mainly based on the nitration of tyrosine by ONOO[−] and posterior detection of formed 3-nitrotyrosine by immunochemical or chromatographic techniques. This assay was used by Girard *et al.*⁵² who developed a method to detect ONOO[−] anions in alkaline buffered solution treated by He/N₂ (1%) plasma presuming that ONOO[−] is formed from O₂•[−] and •NO (eqn (1)). Based on the absorption measurements and molar extinction coefficients of the system NO₂[−]/HO₂[−]/ONOO[−], ~20 μM of ONOO[−] was calculated after 5 min plasma treatment. This result was validated by an assay based on monitoring 3-nitrotyrosine adducts by absorption spectroscopy following the reaction of •NO₂ formed during ONOO[−] decomposition with L-tyrosine in PBS treated by plasma. Furthermore, UV absorbance is used for detection in separation techniques. ONOO[−] anions in aqueous solution give a spectrum with the maximum absorbance at 302 nm (ε = 1670 M^{−1} cm^{−1}), but also at 322 nm (ε = 1308 M^{−1} cm^{−1}).⁴⁸ However, in aqueous solutions, especially PAW containing ONOO[−] and much higher concentrations of NO₃[−] (with absorption at ~300–302 nm), the use of UV spectrometry may be problematic due to the overlap of their spectra. ONOOH has an absorption maximum at ~240–250 nm (ε = 770–700 M^{−1} cm^{−1}) with no appreciable absorption above

300 nm.^{53,54} Oehmingen *et al.*⁵⁰ attempted to prove the formation of ONOO⁻/ONOOH by absorption measurements of plasma activated saline, or solutions of H₂O₂ and NaNO₂ and their mixture at acidic pH. They observed the appearance of a new absorption maximum at 302.5 nm after mixing these components at acidic pH, which was attributed to the formation of ONOO⁻/ONOOH by addition of NO₂⁻ to acidic H₂O₂ solution. The same absorption maximum at 302 nm was detected in plasma activated saline after treatment by surface-DBD in atmospheric air.

Another approach based on using phenol as a reactive species indicator was used by Lukes *et al.*³⁹ and Laurita *et al.*²⁶ Hydroxylated phenol degradation products and nitrated degradation by-products were detected after direct treatment of phenol solution by pulsed or DBD discharge above the liquid surface. The same degradation products were formed in the phenol solution mixed only with PAW due to the post-discharge induced chemical processes. All detected degradation products gave clear evidence of the formation of •NO₂, •NO and •OH radicals at the gas-liquid interface and in the bulk liquid, from which •OH and •NO₂ are known to be products of ONOOH decay chemistry. Additionally, a chemical kinetics analysis of post-discharge chemical processes in PAW as well as in artificial PAW simulated by a respective mixture of NO₂⁻ and H₂O₂ was performed by Lukes *et al.*³⁹ From the kinetics between H₂O₂ and NO₂⁻ according to the reaction (eqn (3)), the formation rate of ONOOH in PAW was calculated in the range 10⁻⁸–10⁻⁹ Ms⁻¹ for given experimental conditions.

Furthermore, electrochemical sensors or oxidation of chromophores and fluorescent and chemiluminescent probes by peroxynitrites are used for *in vivo* detection under physiological conditions, *e.g.* dihydrorhodamine 123, dichlorodihydrofluorescein, luminol or novel fluorescent probes.^{55–59} Fluorescence detection of peroxynitrites by folic acid in PAW activated by an atmospheric pressure plasma jet was used by Zhou *et al.*²⁸ Based on the calibration the rate constant of peroxynitrite formation was determined to be $\sim 1.6 \times 10^{-8} \text{ M s}^{-1}$. However, it must be noted that fluorescence methods have some limitations which have to be considered in the evaluation of experimental results. Because of their possible cross-reactivity, knowledge of the reactivity of the used dyes with different oxidants and the proper use of scavengers and inhibitors is required.^{60,61} Similar to electrochemical sensors, some fluorescent probes are pH-dependent, which may be a limiting factor, especially for their use in acidified PAW.

The present study addresses this possibility of qualitative detection of the peroxynitrite/peroxynitrous acid couple (ONOO⁻/ONOOH) in air atmospheric plasma activated solutions by means of fluorescence spectroscopy using 2,7-dichlorodihydrofluorescein diacetate (H₂DCFDA) fluorescent dye. The study is based on the preliminary results presented in our previous paper,³⁸ where the H₂DCFDA fluorescent dye was used to detect ONOO⁻/ONOOH in buffered and non-buffered solution treated by air transient spark (TS) discharge with electrospray (ES). First, we showed that the sensitivity of H₂DCFDA toward H₂O₂ (at a similar concentration and pH to that produced in PAW) compared to its sensitivity toward the PAW was negligible, therefore refuting the effects of

H₂O₂ on the H₂DCFDA fluorescence signal. Furthermore, the measured fluorescence signal in PAW was significantly higher than the signal induced in plasma activated buffered solution. These results were also directly correlated with the strong bactericidal efficacy and plasma induced oxidative stress on bacterial cell suspensions in PAW compared to plasma activated buffered solution.

The 2,7-dichlorodihydrofluorescein diacetate (H₂DCFDA) fluorescent dye is one of the fluorescein derivatives and has been used as an intracellular marker of oxidative stress or intracellular reactive oxygen species. H₂DCFDA is one of the most discussed fluorescent dyes for peroxynitrite detection. The state-of-the-art on the specificity of this dye brings various conclusions that are affected by the conditions, whether the dye is used in a cell-free system or for intracellular measurements. The possible interferences, mainly for intracellular measurements, were reviewed, for instance in ref. 60–62. The dye was initially described as an assay for the measurement of H₂O₂ in the presence of peroxidase.⁶³ Additionally, it was also found that this dye shows varied sensitivity to reactive species, such as ONOO⁻, •OH, O₂•⁻, •NO₂ or •OOR.^{64–67} According to Kalyanaraman *et al.*,⁶⁰ H₂DCFDA may be used as a redox indicator probe that responds to changes in intracellular iron signalling or peroxynitrite formation. Several papers were published about the much higher sensitivity of the dye toward peroxynitrites (either chemically synthesized or simultaneously generated from •NO and O₂•⁻).^{67–69} Regarding the sensitivity of the dye, Possel *et al.*⁶⁷ showed that low peroxynitrite concentrations (1–5 μM) induced a rapid and efficient increase of the fluorescent form of the dye, whereas Hempel *et al.*⁷⁰ or Kooy *et al.*⁶⁹ managed to detect increased fluorescence with even lower peroxynitrite concentrations (<200 nM).

Therefore, after taking into account the positive preliminary results and on the other hand all possible limitations of using the H₂DCFDA fluorescent dye, we focused our investigations on ways to achieve specific detection of ONOO⁻/ONOOH by this dye and employed various RONS scavengers to limit the cross-reactivity of the dye with different RONS present in aqueous solutions activated by air plasmas.

In our experiments, non-buffered or buffered aqueous solutions were treated by cold air plasma generated by TS discharge in ambient air. Solutions were electrosprayed directly through TS discharge to enhance the gas-liquid transfer of reactive species. First, possible cross-reactivity of the H₂DCFDA dye with various RONS, which are typically produced in PAW, was checked. Second, the specificity of various RONS scavengers was investigated with respect to the H₂DCFDA fluorescence response. Third, the fluorescence response of H₂DCFDA was measured in plasma activated aqueous solutions directly after plasma treatment. To prove that ONOO⁻/ONOOH are formed in acidified PAW and they are responsible for the strong fluorescence response of the H₂DCFDA dye, RONS scavengers for H₂O₂ and NO₂⁻, the reactant species of peroxynitrite chemistry, as well as the scavenger of its end-products, were used. Finally, we performed a kinetic study of post-discharge processes in PAW focused on the formation of ONOOH followed by the parallel detection of ONOO⁻/ONOOH with the H₂DCFDA fluorescent dye.

2. Experimental set-up and methods

2.1 Transient spark with water electro spray

The experimental set-up of the water electro spray and discharge plasma system is depicted in Fig. 1. Transient spark (TS) discharge in positive polarity was generated in ambient air at atmospheric pressure in a point-to-plane geometry. TS discharge is a self-pulsing repetitive streamer-to-spark discharge with a very short duration (< 50 ns) of the spark current pulse (~ 25 A) with a typical repetition frequency of ~ 1 kHz.^{38,71,72} The aqueous solutions were injected by a syringe pump NE-300 (Pump Systems) through the high voltage (HV) electrode represented by a hypodermic hollow needle. This allowed the aqueous solutions to flow directly through the active zone of the discharge with a flow rate of 0.5 mL min^{-1} . Furthermore, due to the applied high voltage, an electro spray effect (ES) – a finely nebulizing effect at the needle tip induced by the electric field – occurred.⁷³ Due to micrometric water droplet sizes, this electro spray enhanced the mass transfer of RONS formed in the gaseous plasma into the aqueous solutions. A stainless steel mesh placed above the Petri dish was used as a grounded electrode, in which the electro sprayed water was collected. The inter-electrode spacing between the HV needle tip and the metallic grounded mesh was kept at 10 mm. The discharge voltage was measured by a HV probe Tektronix P6015A and the discharge current was measured by a Rogowski current monitor Pearson Electronics 2877. The electrical parameters were processed and recorded during the experiments by a 200 MHz oscilloscope Tektronix TDS 2024C. Typical current and voltage waveforms of TS discharge with ES, as well as its electrical parameters, were documented in detail in our previous publications.^{9,38}

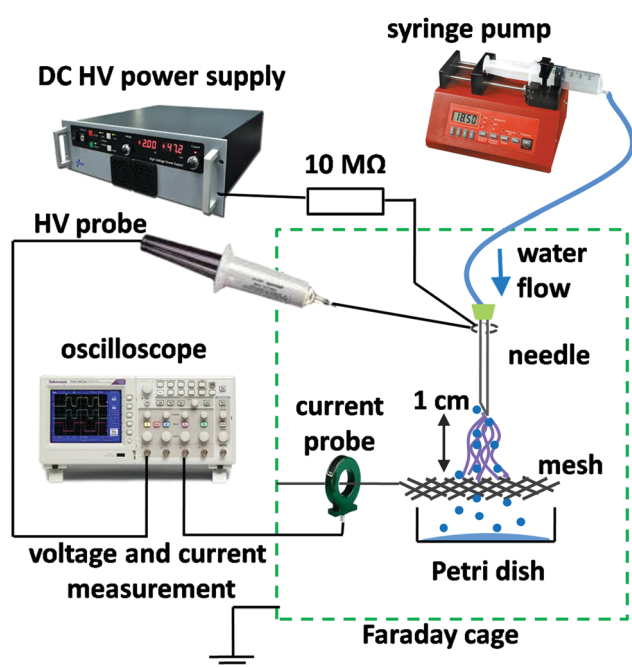


Fig. 1 Experimental set-up of air transient spark discharge with water electro spray.

2.2 Aqueous solutions

The chemical composition and properties of the aqueous solutions (initial pH_i and electrolytic conductivity σ_i , pH after plasma treatment) are listed in Table 1. We used several phosphate aqueous solutions differentiated according to the following parameters:

- Buffering activity – buffered (PB and PBS) and non-buffered (W) solutions.
- pH – acidic (pH ~ 3.2) and neutral (pH 6.9–7.4) solutions.
- Content of chlorine – with Cl (PBS) and without Cl (W and PB).

All aqueous solutions (except PBS) were prepared by dissolution of phosphate salts in Milli-Q water. Weak phosphate solution (denoted as W) was designed as a model solution to mimic the conductivity of tap water and has a similar composition to the phosphate buffered solution (PB). Furthermore, this weak phosphate solution became acidified after plasma treatment unlike PB, which kept the pH thanks to its buffering capacity. We refer to all solutions treated by TS with water electro spray as plasma activated solutions, *i.e.* plasma activated phosphate buffer (PAPB), plasma activated phosphate buffered saline (PAPBS) and plasma activated weak phosphate solution (PAW). Additionally, acidified weak phosphate solution (denoted as acidified W) was used to simulate the acidic environment of PAW without any of the plasma generated RONS present. This solution did not come into contact with the plasma at all and its pH was adjusted to the pH value of fresh PAW treated by TS plasma (*i.e.* pH = 3.2).

2.3 Chemical analyses of plasma activated solutions

H₂DCFDA fluorescence assay. Detection of ONOO⁻/ONOOH was performed by fluorescence spectroscopy using the 2,7-dichlorodihydrofluorescein diacetate (2-(2,7-dichloro-3,6-diacetoxy-9H-xanthen-9-yl)-benzoic acid) (H₂DCFDA) fluorescent dye (Cayman Chemicals). H₂DCFDA represents a non-fluorescent form of the dye. Our samples were represented only by aqueous solutions, therefore the process of chemical deacetylation is required. After deacetylation, still the non-fluorescent form 2,7-dichlorodihydrofluorescein (DCFH) can be very easily oxidized to the highly fluorescent form 2,7-dichlorofluorescein (DCF). A daily fresh working solution of DCFH was prepared according to the assay described in ref. 67. Briefly, the process of deacetylation was provided by hydrolysis with NaOH by mixing 0.5 mL of stock H₂DCFDA solution (1 mM prepared in ethanol) with 2 mL of 0.1 M NaOH solution. The reaction was stopped after 30 minutes incubation at room temperature by adding 7.5 mL of 0.1 M phosphate buffer. By this procedure, 10 mL of 50 μM working solution of DCFH was obtained. Prior to the experiment, a fresh working solution of the dye was prepared. Due to the possible light and oxygen sensitivity, the dye was kept on ice, in the dark, and under an argon atmosphere to minimize autofluorescence. Aqueous samples were mixed with pre-cooled dye directly in 96-well plates (180 μL sample + 20 μL dye, or 170 μL sample + 10 μL scavenger + 20 μL dye, respectively), or in a low volume fluorescence cuvette and

Table 1 Chemical composition and properties of aqueous solutions

Name (abbreviation)	Composition	pH _i	pH	σ _i [mS cm ⁻¹]	Cl
Phosphate buffer (PB)	2 mM Na ₂ HPO ₄ /KH ₂ PO ₄	6.9	6.8	0.56	–
Phosphate buffered saline (PBS)	Dulbecco's PBS w/o Ca, Mg	7.4	7.4	14	+
Phosphate solution (W)	8.5 mM NaH ₂ PO ₄	5	3.2	0.6	–
Acidified phosphate solution (acidified W)	8.5 mM NaH ₂ PO ₄ in diluted H ₃ PO ₄ (1 : 1000)	3.2	–	0.53	–

pH_i – initial pH, pH – pH after plasma treatment, σ_i – initial conductivity, Cl – presence of chlorine.

incubated in the dark at room temperature for 2 minutes.⁶⁹ The fluorescence measurements were performed using a fluorescence spectrometer (Fluorolog[®] 3 (Horiba Scientific)) or fluorescence plate readers (Tecan Infinite M200 Pro (Tecan Group Ltd) and Varioskan[®] Flash (Thermo Scientific)) using an excitation wavelength of 495 nm and observing the fluorescence at 521 nm. To minimize the impact of autooxidation of the dye on the fluorescence signal, we measured the control samples several times per day and then subtracted this fluorescence from each sample.

Aqueous RONS, their detection and scavengers. To distinguish which part of the fluorescence signal is due to which reactive species, the following scavengers of RONS were tested: ebselen (2-phenyl-1,2-benziselenazol-3(2H)-one) (EBS) for ONOO⁻/ONOOH (Cayman Chemicals), catalase (CAT) from bovine liver (EC 1.11.1.6, Sigma-Aldrich) for H₂O₂, taurine (TAU) and hypotaurine (HTAU) for OCl⁻/HOCl (Sigma-Aldrich), and sodium azide (SA) for NO₂⁻ (Sigma-Aldrich). We also used the following RONS as chemicals using bottle solutions: sodium peroxyxynitrite NaONOO (Cayman Chemical) – 1 mM aliquots in 0.3 M NaOH were stored at –70 °C, further diluted in the above mentioned pre-cooled aqueous solutions as needed prior to each experiment, and stored on ice; hydrogen peroxide (Sigma-Aldrich), sodium hypochlorite (Sigma-Aldrich), and sodium nitrite (Cayman Chemical) – all diluted in the above mentioned aqueous solutions as needed; •OH radicals prepared by the Fenton reaction (1 mM FeSO₄ + 10 mM H₂O₂); and superoxide – prepared by dissolution of KO₂ (Merck) in buffered solutions.

Furthermore, in parallel to the ONOO⁻/ONOOH detection in PAW by the H₂DCFDA fluorescent dye, we performed chemical kinetics analysis of the post-discharge processes in PAW. PAW was withdrawn immediately after plasma treatment and cooled down to 10 °C. Cooling of the sample slowed the rate of the post-discharge kinetic processes and allowed us better sampling in the first 30 minutes in the post-treatment time. Samples for hydrogen peroxide, nitrites and peroxyxynitrites were taken 0; 2.5; 5; 7.5; 10; 12.5; 15; 20; 25 and 30 min after plasma treatment.

Aqueous RONS in PAW were measured by the following methods:

- hydrogen peroxide – a colorimetric method, where titanyl ions Ti⁴⁺ react with H₂O₂ in the presence of NaN₃ and create yellow colored pertitanic acid with the absorption maximum at 407 nm⁷⁴ (detection limit ~ 5 μM);
- nitrites – ion chromatography (IC) using the HPLC system Shimadzu LC-Avp with UV (210 nm) and suppressed conductivity detection. The treated samples for ion chromatography

were fixed immediately by phosphate buffer to stop the acidic decomposition of NO₂⁻. Further details can be found in Lukes *et al.*³⁹ (detection limit 0.25 μM);

- •OH radical produced during the Fenton reaction – electron paramagnetic resonance (EPR) spectroscopy using an EMXmicro X-band spectrometer (Bruker BioSpin GmbH., Rheinstetten, Germany) and 100 mM 5-*tert*-butoxycarbonyl-5-methyl-1-pyrroline-*N*-oxide (BMPO) as a spin trap. More details about the EPR procedure can be found in Tresp *et al.*⁷⁵

3. Results and discussion

3.1 Cross-reactivity of H₂DCFDA with various RONS

Air plasmas generate a number of various RONS in plasma activated liquids. Many of these species are known to be strong oxidants,⁴⁵ which may lead to false positive fluorescence signals due to the oxidant-sensitive character of the dye, if it is not specific enough. Besides ONOO⁻/ONOOH, as the species of our interest, the most prominent cross-reactivities may be due to expected high concentrations of H₂O₂ and OCl⁻, or the high fluorescence response of H₂DCFDA to the •OH radical and OCl⁻.⁷⁶ Beside these RONS, we also tested the fluorescence response to O₂^{•-} and NO₂⁻ (expecting that a similar effect will be caused by NO₃⁻). Since we used non-saline buffered solution (PB) with neutral pH (pH 6.9), we can expect that due to the pK_a values the aqueous RONS will be in the following forms: equilibrium of the protonated and the anion form of the ONOO⁻/ONOOH couple (pK_a 6.8), 25% OCl⁻/75% HOCl (pK_a 7.5) and predominantly the anion form of the O₂^{•-}/[•]OOH couple (pK_a 4.8). RONS solutions were freshly prepared at neutral pH and kept on ice. All handling of the ONOO⁻/ONOOH samples was performed carefully to minimize their decomposition (*i.e.* storage at –70 °C, only fresh aliquots were used and each aliquot was thawed only once, all solutions including the dye were pre-cooled and all samples were kept on ice). However, due to the transient character of ONOO⁻/ONOOH and O₂^{•-}/[•]OOH, the real concentrations in the prepared solutions might be actually lower than the originally prepared concentration stated in the figures. Considering this, we did not perform the same type of experiment for the RONS prepared in the more acidic solution. The data in the following figures are plotted as mean values ± SD on a logarithmic scale; each value is obtained from at least 3 independent repetitions. For the above stated reasons, the data represent the qualitative fluorescence response of certain RONS to the dye and they do not represent any calibration curve to calculate the ONOO⁻/ONOOH concentrations in real plasma activated solutions.

Fig. 2 and 3 show the fluorescence responses of the H₂DCFDA dye to the aqueous RONS in different concentration ranges. As can be seen in Fig. 2, the sensitivity of the H₂DCFDA dye to ONOO⁻/ONOOH is much higher (about 1–2 orders of magnitude) than the sensitivity to OCl⁻/HOCl of the same concentrations. Even the low concentrations of ONOO⁻/ONOOH resulted in a higher fluorescence response than the same concentrations of OCl⁻/HOCl. The fluorescence response of the other tested RONS (H₂O₂, NO₂⁻, O₂^{•-}) (Fig. 3) was not significant, even though their typical concentrations in plasma activated solutions are in – hundreds of μM (*i.e.* H₂O₂, NO₂⁻/NO₃⁻).⁷⁷ Additionally the response of H₂DCFDA to H₂O₂ was previously checked up to a 1 mM concentration even in a more acidic environment (pH 2.6) and was found to be insignificant in comparison with the fluorescence induced by PAW.³⁸ In general, H₂O₂ can imply a strong fluorescence response of H₂DCFDA, but only in the presence of the peroxidase enzyme *e.g.* if it is applied intracellularly, which is not our case, or if the peroxidase enzyme is added externally.

A similar cross-reactivity study of the H₂DCFDA dye with various chemically produced aqueous RONS was performed by Setsukinai *et al.*⁷⁶ and the results were adapted by one of the main manufacturers of the dye. They similarly observed a higher fluorescence response to ONOO⁻ than OCl⁻; however the fluorescence response of the dye to H₂O₂ was slightly higher than to OCl⁻. It needs to be mentioned that this experiment was performed for only one concentration point for each RONS (3 μM OCl⁻ and ONOO⁻, 100 μM H₂O₂) and the experimental conditions differed from ours (*e.g.* they used organic solvent, buffered solution and a higher laboratory temperature). Besides the mentioned RONS, other abundant RONS can be formed in plasma activated solutions, *i.e.* •NO, •NO₂, •OH or ozone O₃, which might be eventually responsible for cross-reactivities. From these we can exclude the effects of O₃ (due to its trace concentrations measured in our PAW^{77,78}) and •NO radicals (due to their minimal fluorescence response to the dye reported

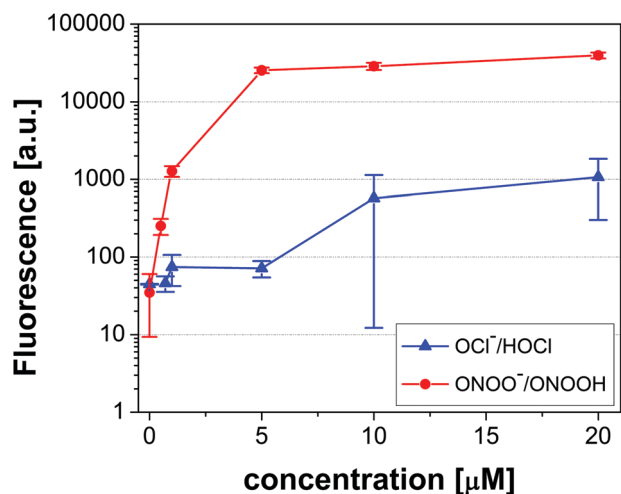


Fig. 2 Fluorescence signal of the H₂DCFDA dye for different concentrations of ONOO⁻/ONOOH and OCl⁻/HOCl in phosphate buffer at pH 6.9. Data are plotted on a logarithmic scale (mean ± SD).

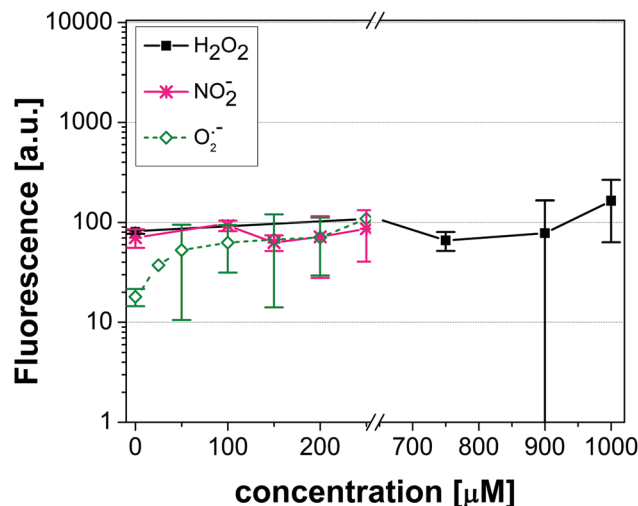


Fig. 3 Fluorescence signal of the H₂DCFDA dye for different concentrations of NO₂⁻, H₂O₂ and O₂^{•-} in phosphate buffer at pH 6.9. Data are plotted on a logarithmic scale (mean ± SD).

in ref. 61, 62 and 76). •NO₂ produced by pulsed radiolysis of aqueous solutions was found to be a more efficient oxidant of the H₂DCFDA dye than the •OH radical according to ref. 64. Unfortunately it was not in our possibilities to check the effect of the •NO₂ contribution to the fluorescence, though this possible effect will be discussed later. Similarly, the effect of the •OH radical will be discussed in the next section.

3.2 Time development of the fluorescence signals of the H₂DCFDA dye with different aqueous RONS and plasma activated solutions

Plasma-induced chemistry in plasma activated liquids depends on the pH. The chemistry between the dye and the reactive species may be affected by the pH, too. In the next step, we measured the evolution of the fluorescence response of the H₂DCFDA dye after mixing with aqueous RONS from the bottle in neutral (PB) and acidic (acidified phosphate solution) pH, and with fresh plasma activated PBS (PAPBS) and phosphate solution (PAW). Fig. 4 shows the time evolution of the fluorescence signal of the H₂DCFDA dye after mixing (at time 0 min with further sampling at each 2 minutes for fluorescence reading) with all plasma activated solutions and various RONS at different pH of the solutions. We compared the response of the dye at neutral initial pH (PAPBS and 10 μM solutions of RONS in PB) and acidic initial pH (PAW and solutions of RONS in acidified W). However, it should be noted that after mixing with the H₂DCFDA dye, even the initial acidic pH of the mixture (PAW or ONOOH) changed to near-neutral values of 6.6–6.7, and PAPBS with the dye increased the pH to ~7.4, thanks to the strong 0.1 M buffered solution of the dye. This means that the pH of all measured samples after mixing with the dye was near-neutral, near the pK_a value of ONOO⁻/ONOOH, and the main difference from the chemical point of view was just the initial pH of the samples (acidic or neutral).

First, the time development of the fluorescence signal of the H₂DCFDA dye with PAPBS *vs.* the solution of ONOO⁻/ONOOH

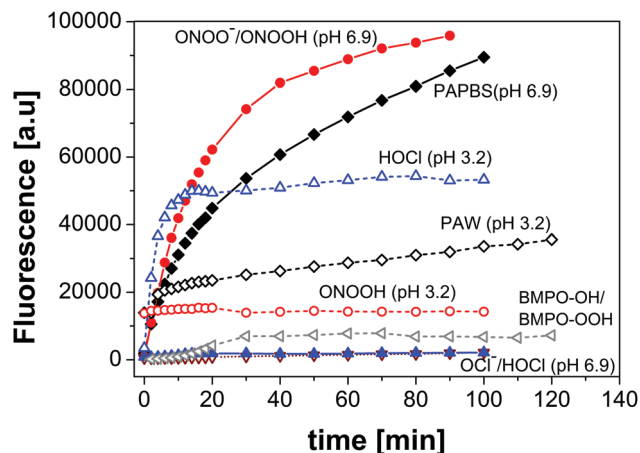


Fig. 4 Time evolution of the H₂DCFDA fluorescence signal for various RONS (10 μM), PAW and PAPBS at different pH. (The pH in the picture refers to the initial pH. The initial acidic pH of the mixture changed to near-neutral values after mixing with the H₂DCFDA dye.) The control (non-treated PBS) fluorescence signal is hidden behind OCl⁻/HOCl (pH 6.9). The 40 μM BMPO-OH spin-trap adduct concentration corresponds to ca. 6.7 mM •OH according to ref. 79.

(pH 6.9) showed a similarity. Although the fluorescence signals induced by the PAPBS and ONOO⁻/ONOOH (pH 6.9) were further growing in time, the fluorescence response of PAW and ONOOH (the predominant form at pH = 3.2) during the first 5 minutes was stronger and reached the maximal intensity. The increase of fluorescence with increasing incubation time may be due to the further oxidation of products. The OCl⁻/HOCl (pH 6.9) induced fluorescence was comparable with the control (non-treated PB + H₂DCFDA dye), but acidified hypochlorites (pH 3.2) induced a strong fluorescence response, probably due to the formation of HOCl (the pK_a of the HOCl/OCl⁻ system is 7.5). Interestingly, the response of the H₂DCFDA dye to •OH radicals produced by the Fenton reaction was considerably lower than to the plasma activated solutions. We used 1 mM FeSO₄ + 10 mM H₂O₂ for the Fenton reaction, which were 10-times higher concentrations than in Setsukinai *et al.*,⁷⁶ who observed the highest fluorescence response of the dye to •OH produced by the Fenton reaction in contrast to our results. Though, as it was mentioned before, their experimental conditions were different and it is not clear how long was the incubation time with the dye, or at which time point of the Fenton reaction the fluorescence was measured. Besides the fluorescence response of the dye, we performed a parallel measurement of the formation of •OH radicals by EPR spectroscopy during the Fenton reaction. By using the BMPO spin trap, we measured both BMPO-OH (~40 μM) and BMPO-OOH (~48 μM) spin-trap adducts, meaning that both •OH and •OOH were formed during the Fenton reaction. Iron Fe²⁺ is oxidized by H₂O₂ to Fe³⁺ in the Fenton reaction forming the •OH radical and hydroxide ion ⁻OH (eqn (6)). The excess of H₂O₂ may lead to its catalytic reduction by Fe³⁺ and form the •OOH radical (eqn (7)).⁸⁰ This reaction is enhanced at acidic pH < 3 with the maximal pseudo-first order rate at pH = 3.⁸¹



We showed that the response of H₂DCFDA is dependent on the pH of the solution and knowing the pH of the working solution is important, because the chemistry pathways of aqueous RONS formed in plasma activated solutions are different at different pH,⁸² which may consequently lead to different results. In ref. 83 it was shown that the oxidation yield due to oxidation by peroxy nitrates is low at pH 2–6 and significantly increases at higher pH (maximum at pH 8.5–9).

3.3 Scavenger cross-reactivities with RONS

To distinguish which part of the fluorescence signal originated from which RONS, we tested scavengers of reactive species specific for certain RONS described earlier in the Experimental section 2.3. However, beside their target RONS, they still may act as scavengers towards other RONS, if they are present. This might cause a problem, since plasma activated solutions are usually mixtures of various highly reactive species, which may affect the specificity of some scavengers.

Because H₂DCFDA was most specific to ONOO⁻/ONOOH and OCl⁻/HOCl, as we have demonstrated above, we decided to test the efficiency of scavengers toward these species and their possible cross-reactivities. According to ref. 84 and 85, the low molecular weight selenium compound – ebselen (EBS) – is described as the most specific scavenger of peroxy nitrates due to the high second-order rate constant of its reaction with peroxy nitrates on the order of 10⁶ M⁻¹ s⁻¹ (2.10⁶ M⁻¹ s⁻¹ at pH ≥ 8). This reaction proceeds even at acidic pH where peroxy nitrous acid represents the predominant form, which is relevant for plasma activated solutions, especially in the case of non-buffered solutions. According to ref. 84, the reaction between EBS and ONOO⁻/ONOOH is substantially faster than the spontaneous decay process of ONOO⁻/ONOOH at physiological pH. We tested the scavenging activity and cross-reactivity of ebselen for solutions of ONOO⁻/ONOOH and OCl⁻/HOCl of the same concentration at neutral pH (prepared in PB). The normalized fluorescence represents the efficiency of the scavenger, where the highest value (1.0) represents no scavenging activity and the lowest value represents the highest scavenging activity of the tested scavenger. Fig. 5 shows that as low as 50 μM EBS scavenged all present ONOO⁻/ONOOH. However, EBS was able to scavenge OCl⁻/HOCl very effectively, too (up to 80–100% depending on the EBS concentration). Due to this fact, EBS should not be used in plasma activated saline solutions as a specific scavenger of ONOO⁻/ONOOH and another more specific scavenger should to be considered in such a case. It needs to be mentioned that EBS may also mimic the properties of the glutathione peroxidase enzyme and act as a reducing agent against H₂O₂.^{86,87} Despite this, the rate constant of their reaction seems to be several orders of magnitude lower,^{86,88} and furthermore, the effect of the cross-reactivity of H₂O₂ on the H₂DCFDA fluorescence was excluded despite high H₂O₂ concentrations.

On the other hand, when working with saline solutions (*e.g.* physiological saline solution or phosphate buffered saline

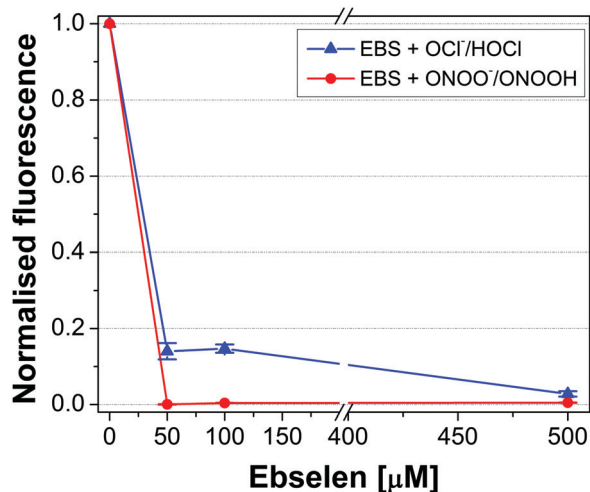


Fig. 5 Scavenging efficiency of ebselen at various concentrations and its cross-reactivity with 10 μM solutions of $\text{ONOO}^-/\text{ONOOH}$ and OCl^-/HOCl prepared in PB (mean \pm SD).

solution typically containing a high concentration of chlorine), which are more suitable for applications in plasma medicine, it may be helpful to scavenge hypochlorites (OCl^-). Therefore, we tested two scavengers – taurine (TAU) and its metabolic precursor hypotaurine (HTAU) – typically acting as *in vitro* and *in vivo* antioxidants.^{89,90} Fig. 6 compares the scavenging efficiencies and cross-reactivities of TAU and HTAU towards $\text{ONOO}^-/\text{ONOOH}$ and OCl^-/HOCl . Both TAU and HTAU are very efficient and have high specificity to OCl^-/HOCl in concentrations above 100 μM . The scavenging activity of HTAU for OCl^-/HOCl increased with increasing concentration and it seemed to be a better scavenger than TAU. Despite this, both TAU and HTAU do not seem to be fully specific for OCl^-/HOCl because of their ability to scavenge also $\text{ONOO}^-/\text{ONOOH}$ (40–60% depending on the scavenger), which was also shown by Oliveira

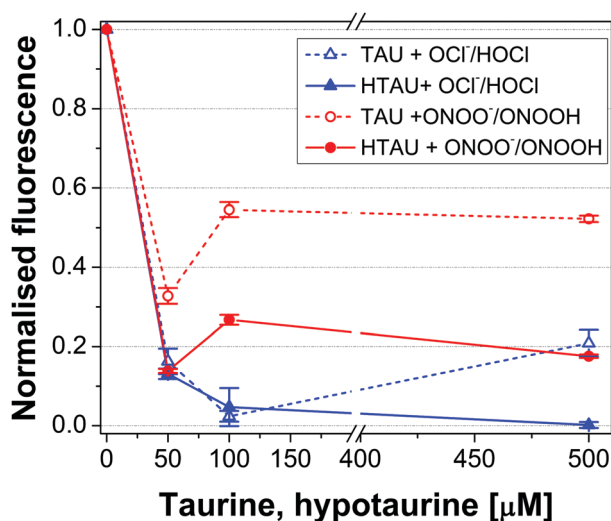


Fig. 6 Scavenging efficiencies of taurine and hypotaurine at various concentrations and their cross-reactivities with 10 μM solutions of $\text{ONOO}^-/\text{ONOOH}$ and OCl^-/HOCl prepared in PB (mean \pm SD).

*et al.*⁹⁰ and Fontana *et al.*⁹¹ Furthermore, good scavenging activity of TAU and HTAU against $\bullet\text{OH}$, $\text{O}_2\bullet^-$ and $\bullet\text{NO}$ radicals, but not against H_2O_2 , was previously shown.^{89,90}

3.4 H_2DCFDA measurements in plasma activated solutions with and without scavengers

The efficiencies of scavengers were subsequently tested in the plasma treated solutions (W, PB and PBS) with respect to the fluorescence signal with or without scavengers added directly after plasma treatment before mixing with the H_2DCFDA dye. The addition of scavengers into the plasma treated solutions allowed us to develop the typical plasma-induced chemistry during the treatment without inhibition of any of the chemical pathways by scavenging certain RONS. The used scavengers were aimed at scavenging the reactants or products of $\text{ONOO}^-/\text{ONOOH}$ formation in plasma activated solutions: catalase (CAT) scavenging H_2O_2 , sodium azide (SA) scavenging NO_2^- and ebselen (EBS) scavenging $\text{ONOO}^-/\text{ONOOH}$. All scavengers were first mixed with the plasma treated solutions and after ~ 30 seconds the pre-cooled H_2DCFDA dye was added according to the procedure.

The fluorescence response of H_2DCFDA to the plasma activated solutions (PAW, PAPB, and PAPBS) without added scavengers is shown in Fig. 7. The observed fluorescence intensity was considerably higher in PAW than in the plasma activated buffered solutions (PAPB and PAPBS).

It is known that the formation of H_2O_2 , NO_2^- and NO_3^- along with acidification (for our PAW the final pH was typically 3.2) takes place in PAW.^{35,36,38,39} These conditions lead to the formation of predominantly ($>99\%$) the protonated form of peroxynitrites (ONOOH) by the reaction of H_2O_2 and NO_2^- according to eqn (3).^{38,39} The same RONS are also formed in buffered solutions, however, the pH of the solution defines the form and the preferred pathway of $\text{ONOO}^-/\text{ONOOH}$ couple formation, as well as their reaction rates. Additionally, our weak phosphate solution (W) and phosphate buffer (PB) do not

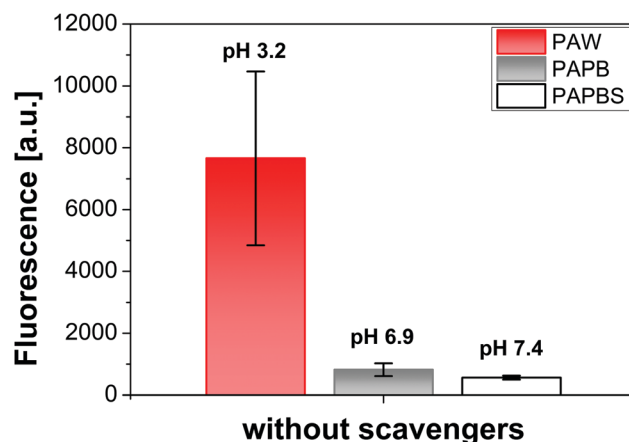


Fig. 7 Fluorescence response of H_2DCFDA to plasma activated aqueous solutions without added RONS scavengers (mean \pm SD). pH values of the solutions after plasma treatment are shown. The final pH after adding the H_2DCFDA dye into PAW was neutralized to values around 6.6–6.7.

contain any chlorine. Therefore the possible formation of OCl^-/HOCl in PAW and PAPB and their effects on the fluorescence were precluded.

In ref. 82 it was shown that the 2nd order rate constant $k_{\text{H}_2\text{O}_2, \text{NO}_2^-}$ of ONOOH formation from H_2O_2 and NO_2^- increased linearly with increasing acidity (*i.e.* an increasing concentration of H^+ ions) of PAW. In neutral solutions (PAPB and PAPBS) the rate constant for eqn (3) can be several orders of magnitude lower (the reaction progresses slower), and additionally the formation of ONOO^- from $\text{O}_2^{\bullet-}$ and $\bullet\text{NO}$ (eqn (1)) may probably take place.⁶ Considering that the concentrations of the origin RONS *i.e.* H_2O_2 and NO_2^- for eqn (3) are typically in – hundreds of μM ranges,^{38,39,77} $\text{O}_2^{\bullet-}$ and $\bullet\text{NO}$ can be expected to be much lower (according to ref. 92 $\bullet\text{NO}$ in PBS treated by spark discharge was in the range – hundreds of nM) in plasma activated buffered solutions (although we have not measured these radicals in our system yet). Despite the rate constant of ONOO^- formation (eqn (1)) being much faster ($\sim 10^9\text{--}10^7 \text{ M}^{-1} \text{ s}^{-1}$) at neutral pH,^{1–3} stronger formation of ONOOH in acidified PAW can be expected. When the sample is mixed with the H_2DCFDA dye, the strong buffer used for the dye preparation buffers the pH of the sample to about neutral values (especially the pH of PAW changed from 3.2 to $\sim 6.6\text{--}6.7$ as was mentioned before). This pH is very close to the pK_a of the $\text{ONOO}^-/\text{ONOOH}$ couple and therefore a significant part of ONOOH will be dissociated into ONOO^- anions. The neutral pH also partially prolongs their life-time. Our measurement procedure involves two minute incubation with the dye, during which the peroxynitrite chemistry can possibly still proceed and oxidize the dye, even though much more slowly due to the neutralized pH. This may explain the significantly lower fluorescence signals in both buffered solutions (PAPB and PAPBS) due to the higher pH compared to the acidic PAW.

In addition, in PAPBS the signal might be not only due to $\text{ONOO}^-/\text{ONOOH}$, but also OCl^-/HOCl if they are being formed.⁹³ Similarly, as we mentioned previously, $\bullet\text{NO}_2$, which is formed due to the acidified decay of ONOOH in PAW, can act as an efficient oxidant of the dye. Therefore, its contribution to the fluorescence signal should be considered, although currently it was not in our possibilities to verify.

By using RONS scavengers we tried to prove that the predominant ONOOH formation is responsible for the strong fluorescence signal of the H_2DCFDA dye in PAW (Fig. 8). Certain specific scavengers can eliminate the signal by scavenging of either the reactants or the product of the reaction of ONOOH formation (eqn (3)). At first, the addition of EBS (100 μM) into PAW significantly decreased the fluorescence signal. We expected that the missing part of the fluorescence signal in PAW is due to the scavenged ONOOH . The remaining signal is probably due to some weak cross-reactivities of other reactive species and autofluorescence. By addition of CAT (2 units per mL) into PAW we observed a significant decrease of the H_2DCFDA fluorescence intensity. We expect that CAT scavenged H_2O_2 needed for the formation of ONOOH , and therefore no or a minimal concentration of ONOOH was formed. In the same manner, we used SA (3.3 mM) as a scavenger of NO_2^- .

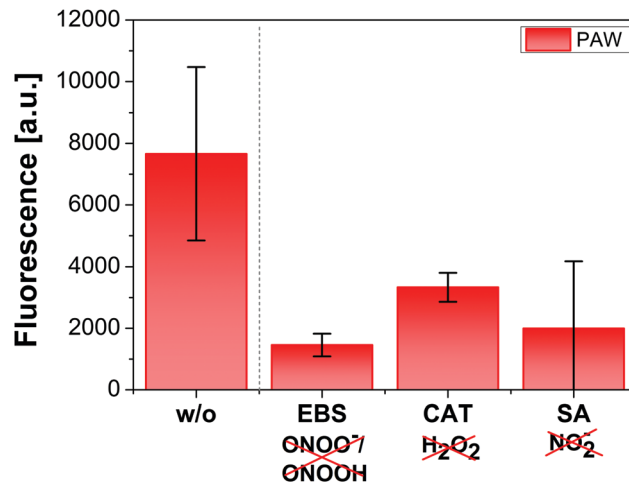


Fig. 8 Comparison of the fluorescence response of H_2DCFDA to PAW without (w/o) and with added RONS scavengers (EBS – ebselen, CAT – catalase, SA – sodium azide), (mean \pm SD).

We observed a similar decrease of the fluorescence signal due to the scavenging of NO_2^- as one of the reactants needed for ONOOH formation. In both cases, after removal of H_2O_2 or NO_2^- by scavengers, the decrease of the fluorescence signal is due to the absence of ONOOH . This result supported the assumption that the fluorescence signal of H_2DCFDA in PAW is caused by $\text{ONOO}^-/\text{ONOOH}$ formation, which also continues in PAW in the post-treatment time. In addition, the peroxynitrite mediated oxidation of the H_2DCFDA dye is not based on the formation of free $\bullet\text{OH}$ radicals as decay products according to Kooy *et al.*⁶⁹ and Glebska *et al.*,⁸³ but it appears to be due to a direct reaction of the conjugated ONOOH with the dye.

Plasma induced chemistry in plasma activated liquids does not represent steady state conditions, but ongoing processes. The chemical instability of ONOOH at acidic pH (eqn (4) and (5)) is also responsible for the high variability of the fluorescence detection in PAW (the standard deviation is about $\pm 30\%$). Considering also the sampling post plasma treatment, longer incubation time and no steady state of ONOOH , the H_2DCFDA assay is not well-suited for “live” measurements of $\text{ONOO}^-/\text{ONOOH}$.

3.5 Simultaneous detection of peroxynitrite/peroxynitrous acid in PAW by H_2DCFDA fluorescence and by a kinetic study of the post-discharge chemistry

In parallel to the detection of $\text{ONOO}^-/\text{ONOOH}$ in PAW by H_2DCFDA fluorescence, we performed a kinetic study of the post-discharge processes.³⁹ TS air plasma activated water (*i.e.* weak phosphate solution) was withdrawn immediately after plasma treatment and H_2O_2 , NO_2^- , and $\text{ONOO}^-/\text{ONOOH}$ were measured at specific post-discharge times up to 30 min post plasma treatment. Although peroxynitrite chemistry typically started during the plasma treatment, in this case we focused on the peroxynitrite chemistry in PAW proceeding independently without plasma action. At first the kinetic evolution of NO_2^- and H_2O_2 (Fig. 9) showed an exponential decrease of their

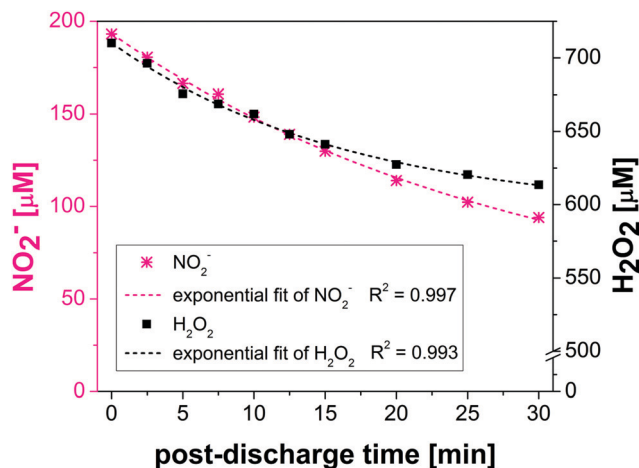


Fig. 9 Post-discharge kinetic evolution of nitrites and hydrogen peroxide in PAW in the post-discharge time.

concentrations in PAW, as a result of the post-discharge processes due to the continuous formation of the predominant ONOOH form (eqn (3)).^{39,46}

According to ref. 39 the formation rate of ONOOH can be written as (eqn (8))

$$r_{\text{ONOOH}} = \frac{d[\text{ONOOH}]}{dt} = k[\text{H}^+][\text{H}_2\text{O}_2][\text{NO}_2^-], \quad (8)$$

where k is the third-order rate constant for the reaction (eqn (3)). There is a strong dependence of k on the H^+ concentration (*i.e.* pH) in the reaction (eqn (3)). However, in the buffered solution the overall third-order kinetics of the reaction (eqn (3)) can be simplified to pseudo-second order under the assumption that the concentration of H^+ ions remains constant. Then the expression (eqn (8)) can be rewritten as (eqn (9))

$$-\frac{d[\text{H}_2\text{O}_2]}{dt} = k_{\text{H}_2\text{O}_2, \text{NO}_2^-} [\text{H}_2\text{O}_2][\text{NO}_2^-], \quad (9)$$

where $k_{\text{H}_2\text{O}_2, \text{NO}_2^-} = k[\text{H}^+]$ is the pseudo-second-order rate constant for the reaction between H_2O_2 and NO_2^- . The integration of the equation (eqn (9)) from time $t = 0$ to t gives (eqn (10))

$$\ln \frac{[\text{NO}_2^-]_t [\text{H}_2\text{O}_2]_0}{[\text{H}_2\text{O}_2]_t [\text{NO}_2^-]_0} = k_{\text{H}_2\text{O}_2, \text{NO}_2^-} ([\text{NO}_2^-]_0 - [\text{H}_2\text{O}_2]_0) t. \quad (10)$$

Based on our kinetic study of post-discharge processes we experimentally determined the pseudo-second order rate constant $k_{\text{H}_2\text{O}_2, \text{NO}_2^-} = 0.635 \text{ M}^{-1} \text{ s}^{-1}$ for given experimental conditions (pH 3.2; 10 °C), as well as the third-order rate constant $k_{\text{ONOOH}} = 1.01 \times 10^{-3} \text{ M}^{-2} \text{ s}^{-1}$ for the reaction (eqn (3)) using the calculated concentration of $[\text{H}^+] = 6.31 \times 10^{-4} \text{ M}$ for pH 3.2. From eqn (8) we determined the rate of formation of peroxyntitrous acid r_{ONOOH} in PAW (pH 3.2) for each time point from 0 to 30 min post plasma treatment. The initial rate of ONOOH formation in fresh PAW ($t = 0$ min represents the time point at which the PAW was withdrawn from the plasma) was determined to be $r_{\text{ONOOH}} = 87 \text{ nM s}^{-1}$. As can be seen, the rate decreased exponentially in the post-discharge time (Fig. 10) due to the consumption of nitrites

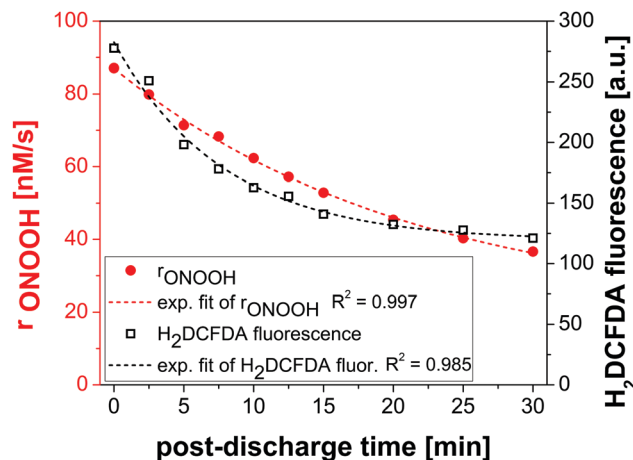


Fig. 10 Parallel detection of ONOO⁻/ONOOH in PAW in the post-discharge time by the fluorescent dye H₂DCFDA and by the kinetic study of the ONOOH formation rate r_{ONOOH} .

and hydrogen peroxide needed for ONOOH formation (shown in Fig. 9).

In the second step, the time dependent evolution of the ONOOH formation rate r_{ONOOH} in PAW was compared with the time evolution of the measured fluorescence signal of H₂DCFDA in PAW in the post-discharge time. The trend of the H₂DCFDA fluorescence signal showed a very similar decreasing exponential trend as a result of the decrease of the ONOOH concentration due to its acidic decomposition into $\cdot\text{OH}$ and $\cdot\text{NO}_2$ radicals and NO_3^- (eqn (4) and (5)) in PAW in the post-discharge time. As can be seen in Fig. 10, there is a very good agreement in the detection of ONOO⁻/ONOOH by these two methods. Hence we calculated the formation rate of ONOOH in the $\sim\text{nM}$ range; the actual concentrations of ONOOH in PAW during the plasma treatment might be higher (ONOOH is continuously formed and decays). As was mentioned before, this technique is not suitable for “live” detection; more precisely this assay involves both ONOOH formation and decay processes and averages them during the incubation time with the fluorescent dye. Despite the low expected steady-state concentration of ONOO⁻/ONOOH in PAW due to their short life-time, the H₂DCFDA dye effectively detected these low concentrations, showed its great sensitivity and can serve as a qualitative method for ONOO⁻/ONOOH detection in different types of PAWs.

4. Conclusions

Peroxyntitrites/peroxyntitrous acid are known as one of the key antimicrobial agents in cold air plasma activated water and aqueous solutions. Because of the presence of various RONS in PAW, possible cross-reactivities, and especially their short life-time, make the detection of ONOO⁻/ONOOH difficult. The reaction chemistry at different pH takes place along different pathways and it is very important to consider all limitations of every method used for the detection of RONS in PAW and

plasma activated solutions. In this work, we showed a new approach to the qualitative detection of ONOO⁻/ONOOH in acidified PAW by using the fluorescent dye 2,7-dichlorodihydrofluorescein diacetate. We demonstrated that in plasma activated solutions without the presence of Cl⁻, thus prohibiting formation of hypochlorite anions (OCl⁻) or hypochlorous acid (HOCl), the H₂DCFDA fluorescence signal can be attributed primarily to ONOO⁻/ONOOH formed primarily *via* the reaction of nitrites and hydrogen peroxide in PAW. If careful considerations are made towards the conditions of the plasma treatment and the treated solution, fluorescence detection of ONOO⁻/ONOOH is a very promising method for the detection of these crucial RONS in the domain of plasmas with liquids and plasma medicine.

Conflicts of interest

There are no conflicts to declare.

Appendix

Table 2 List of used abbreviations

Aqueous solutions	
PB	Phosphate buffer
PAPB	Plasma activated phosphate buffer
PBS	Phosphate buffered saline
PAPBS	Plasma activated phosphate buffered saline
W	Weak phosphate solution
PAW	Plasma activated weak phosphate solution
Scavengers of reactive species	
CAT	Catalase
EBS	Ebselen
HTAU	Hypotaurine
SA	Sodium azide
TAU	Taurine
Others	
DCF	2,7-Dichlorofluorescein
DCFH	2,7-Dichlorodihydrofluorescein
ES	Electrospray
EPR	Electron paramagnetic spectroscopy
H ₂ DCFDA	2,7-Dichlorodihydrofluorescein diacetate
HPLC	High performance liquid chromatography
HV	High voltage
RONS	Reactive oxygen and nitrogen species
TS	Transient spark

Acknowledgements

This work was supported by Slovak Research and Development Agency APVV-0134-12, APVV-17-0382 and Comenius University in Bratislava. The research stays of BT at INP Greifswald and the ZIK plasmatis in the research group of SR were funded by the German Federal Ministry of Education and Research (BMBF) (Grant No. 03Z22DN12) and by the COST Action TD1208 – Electrical Discharges with Liquids for Future Applications. The research stay of BT at IPP Prague in the group of PL was funded

by COST Action TD1208 – Electrical Discharges with Liquids for Future Applications, Ministry of Education, Youth and Sports of the Czech Republic (project COST LD 14080), and by the Czech Science Foundation (GACR) – project No. 19-25026S. HJ additionally acknowledges funding from the German Federal Ministry of Education and Research (BMBF) (Grant No. 03Z22DN12).

References

- W. H. Koppenol, The chemistry of peroxyxynitrite, a biological toxin, *Quim. Nova*, 1998, **21**, 326–331.
- C. Szabó, H. Ischiropoulos and R. Radi, Peroxyxynitrite: biochemistry, pathophysiology and development of therapeutics, *Nat. Rev. Drug Discovery*, 2007, **6**, 662–680.
- J. R. Lancaster Jr., Nitroxidative, nitrosative, and nitrative stress: kinetic predictions of reactive nitrogen species chemistry under biological conditions, *Chem. Res. Toxicol.*, 2006, **19**, 1160–1174.
- A. Denicola, J. M. Souza and R. Radi, Diffusion of peroxyxynitrite across erythrocyte membranes, *Proc. Natl. Acad. Sci. U. S. A.*, 1998, **95**, 3566–3571.
- M. P. Murphy, M. A. Packer, J. L. Scarlett and S. W. Martin, Peroxyxynitrite: a biologically significant oxidant, *Gen. Pharmacol.*, 1998, **31**, 179–186.
- R. Radi, A. Denicola, B. Alvarez, G. Ferrer-Sueta and H. Rubbo, The biological chemistry of peroxyxynitrite, in *Nitric Oxide. Biology and Pathobiology*, ed. J. Ignarro Louis, Academic Press, 2000, ch. 4.
- G. Ferrer-Sueta and R. Radi, Chemical biology of peroxyxynitrite: kinetics, diffusion, and radicals, *ACS Chem. Biol.*, 2009, **4**, 161–177.
- S. Carballal, S. Bartesaghi and R. Radi, Kinetic and mechanistic considerations to assess the biological fate of peroxyxynitrite, *Biochim. Biophys. Acta*, 2014, **1840**, 768–780.
- K. Hensel, K. Kučerová, B. Tarabová, M. Janda, Z. Machala, K. Sano, C. T. Mihai, M. Ciorpac, L. D. Gorgan, R. Jijie, V. Pohoata and I. Topala, Effects of air transient spark discharge and helium plasma jet on water, bacteria, cells, and biomolecules, *Biointerphases*, 2015, **10**, 29515.
- N. Kaushik, N. Kumar, C. H. Kim, N. K. Kaushik and E. H. Choi, Dielectric barrier discharge plasma efficiently delivers an apoptotic response in human monocytic lymphoma, *Plasma Processes Polym.*, 2014, **11**, 1175–1187.
- N. Barekzi and M. Laroussi, Effects of low temperature plasmas on cancer cells, *Plasma Processes Polym.*, 2013, **10**, 1039–1050.
- H. Tanaka, K. Ishikawa, M. Mizuno, S. Toyokuni, H. Kajiyama, F. Kikkawa, H.-R. Metelmann and M. Hori, State of the art in medical applications using non-thermal atmospheric pressure plasma, *Rev. Mod. Plasma Phys.*, 2017, **1**, 1–89.
- J. Julák and V. Scholtz, Decontamination of human skin by low-temperature plasma produced by cometary discharge, *Clin. Plasma Med.*, 2013, **1**, 31–34.
- O. J. Cahill, T. Claro, A. A. Cafolla, N. T. Stevens, S. Daniels and H. Humphreys, Decontamination of Hospital Surfaces

- With Multijet Cold Plasma: A Method to Enhance Infection Prevention and Control?, *Infect. Control Hosp. Epidemiol.*, 2017, **38**, 1182–1187.
- 15 U. Schnabel, T. Maucher, J. Köhnlein, W. Volkwein, R. Niquet, I. Trick, M. Stieber, M. Müller, H. P. Werner, J. Ehlbeck, C. Oehr and K. D. Weltmann, Multicentre trials for decontamination of fine-lumen PTFE tubes loaded with bacterial endospores by low and atmospheric pressure plasma, *Plasma Processes Polym.*, 2012, **9**, 37–47.
- 16 L. Jablonowski, I. Koban, M. H. Berg, E. Kindel, K. Duske, K. Schröder, K. D. Weltmann and T. Kocher, Elimination of *E. faecalis* by a new non-thermal atmospheric pressure plasma handheld device for endodontic treatment. A preliminary investigation, *Plasma Processes Polym.*, 2013, **10**, 499–505.
- 17 I. Koban, B. Holtfreter, N. O. Hübner, R. Matthes, R. Sietmann, E. Kindel, K. D. Weltmann, A. Welk, A. Kramer and T. Kocher, Antimicrobial efficacy of non-thermal plasma in comparison to chlorhexidine against dental biofilms on titanium discs *in vitro* – Proof of principle experiment, *J. Clin. Periodontol.*, 2011, **38**, 956–965.
- 18 R. Wang, H. Zhou, P. Sun, H. Wu and J. Pan, The Effect of an Atmospheric Pressure, DC Nonthermal Plasma Microjet on Tooth Root Canal, Dentinal Tubules Infection and Reinfection Prevention, *Plasma Med.*, 2011, **1**, 143–155.
- 19 A. Kramer, J. Lademann, C. Bender, A. Sckell, B. Hartmann, S. Münch, P. Hinz, A. Ekkernkamp, R. Matthes, I. Koban, I. Partecke, C. D. Heidecke, K. Masur, S. Reuter, K. D. Weltmann, S. Koch and O. Assadian, Suitability of tissue tolerable plasmas (TTP) for the management of chronic wounds, *Clin. Plasma Med.*, 2013, **1**, 11–18.
- 20 B. Haertel, T. von Woedtke, K. D. Weltmann and U. Lindequist, Non-thermal atmospheric-pressure plasma possible application in wound healing, *Biomol. Ther.*, 2014, **22**, 477–490.
- 21 G. Isbary, J. L. Zimmermann, T. Shimizu, Y. F. Li, G. E. Morfill, H. M. Thomas, B. Steffes, J. Heinlin, S. Karrer and W. Stolz, Non-thermal plasma—More than five years of clinical experience, *Clin. Plasma Med.*, 2013, **1**, 19–23.
- 22 V. Miller, A. Lin and A. Fridman, Why Target Immune Cells for Plasma Treatment of Cancer, *Plasma Chem. Plasma Process.*, 2016, **36**, 259–268.
- 23 H.-R. Metelmann, D. S. Nedrelov, C. Seebauer, M. Schuster, T. von Woedtke, K.-D. Weltmann, S. Kindler, P. H. Metelmann, S. E. Finkelstein, D. D. Von Hoff and F. Podmelle, Head and neck cancer treatment and physical plasma, *Clin. Plasma Med.*, 2015, **3**, 17–23.
- 24 D. B. Graves, Reactive species from cold atmospheric plasma: implications for cancer therapy, *Plasma Processes Polym.*, 2014, **11**, 1120–1127.
- 25 M. J. Traylor, M. J. Pavlovich, S. Karim, P. Hait, Y. Sakiyama, D. S. Clark and D. B. Graves, Long-term antibacterial efficacy of air plasma-activated water, *J. Phys. D: Appl. Phys.*, 2011, **44**, 472001.
- 26 R. Laurita, D. Barbieri, M. Gherardi, V. Colombo and P. Lukes, Chemical analysis of reactive species and antimicrobial activity of water treated by nanosecond pulsed DBD air plasma, *Clin. Plasma Med.*, 2015, **3**, 53–61.
- 27 S. Ikawa, A. Tani, Y. Nakashima and K. Kitano, Physicochemical properties of bactericidal plasma-treated water, *J. Phys. D: Appl. Phys.*, 2016, **49**, 425401.
- 28 R. Zhou, R. Zhou, K. Prasad, Z. Fang, R. Speight, K. Bazaka and K. (Ken) Ostrikov, Cold atmospheric plasma activated water as a prospective disinfectant: the crucial role of peroxyxynitrite, *Green Chem.*, 2018, **20**, 5276–5284.
- 29 N. Kurake, H. Tanaka, K. Ishikawa, T. Kondo, M. Sekine, K. Nakamura, H. Kajiyama, F. Kikkawa, M. Mizuno and M. Hori, Cell survival of glioblastoma grown in medium containing hydrogen peroxide and/or nitrite, or in plasma-activated medium, *Arch. Biochem. Biophys.*, 2016, **605**, 102–108.
- 30 K. R. Liedtke, S. Bekeschus, A. Kaeding, C. Hackbarth, J.-P. Kuehn, C.-D. Heidecke, W. von Bernstorff, T. von Woedtke and L. I. Partecke, Non-thermal plasma-treated solution demonstrates antitumor activity against pancreatic cancer cells *in vitro* and *in vivo*, *Sci. Rep.*, 2017, **7**, 8319.
- 31 D. Yan, A. Talbot, N. Nourmohammadi, X. Cheng, J. Canady, J. Sherman and M. Keidar, Principles of using Cold Atmospheric Plasma Stimulated Media for Cancer Treatment, *Sci. Rep.*, 2016, **5**, 17.
- 32 P. J. Bruggeman, M. J. Kushner, B. R. Locke, J. G. E. Gardeniers, W. G. Graham, D. B. Graves, R. C. H. M. Hofman-Caris, D. Maric, J. P. Reid, E. Ceriani, D. Fernandez Rivas, J. E. Foster, S. C. Garrick, Y. Gorbanev, S. Hamaguchi, F. Iza, H. Jablonowski, E. Klimova, J. Kolb, F. Krma, P. Lukes, Z. Machala, I. Marinov, D. Mariotti, S. Mededovic Thagard, D. Minakata, E. C. Neyts, J. Pawlat, Z. L. Petrovic, R. Pflieger, S. Reuter, D. C. Schram, S. Schröter, M. Shiraiwa, B. Tarabová, P. A. Tsai, J. R. R. Verlet, T. von Woedtke, K. R. Wilson, K. Yasui and G. Zvereva, Plasma-liquid interactions: a review and roadmap, *Plasma Sources Sci. Technol.*, 2016, **25**, 53002.
- 33 H. Jablonowski and T. von Woedtke, Research on plasma medicine-relevant plasma-liquid interaction: what happened in the past five years?, *Clin. Plasma Med.*, 2015, **3**, 42–52.
- 34 J. L. Brisset and J. Pawlat, Chemical Effects of Air Plasma Species on Aqueous Solutes in Direct and Delayed Exposure Modes: Discharge, Post-discharge and Plasma Activated Water, *Plasma Chem. Plasma Process.*, 2016, **36**, 355–381.
- 35 M. Naïtali, G. Kamgang-Youbi, J.-M. Herry, M.-N. Bellon-Fontaine and J.-L. Brisset, Combined Effects of Long-Living Chemical Species during Microbial Inactivation Using Atmospheric Plasma-Treated Water, *Appl. Environ. Microbiol.*, 2010, **76**, 7662–7664.
- 36 K. Oehmigen, M. Hähnel, R. Brandenburg, C. Wilke, K. D. Weltmann and T. von Woedtke, The role of acidification for antimicrobial activity of atmospheric pressure plasma in liquids, *Plasma Processes Polym.*, 2010, **7**, 250–257.
- 37 J. Julák, V. Scholtz, S. Kotúčová and O. Janoušková, The persistent microbicidal effect in water exposed to the corona discharge, *Phys. Medica*, 2012, **28**, 230–239.
- 38 Z. Machala, B. Tarabova, K. Hensel, E. Spetlikova, L. Sikurova and P. Lukes, Formation of ROS and RNS in

- water electro-sprayed through transient spark discharge in air and their bactericidal effects, *Plasma Processes Polym.*, 2013, **10**, 649–659.
- 39 P. Lukes, E. Dolezalova, I. Sisrova and M. Clupek, Aqueous-phase chemistry and bactericidal effects from an air discharge plasma in contact with water: evidence for the formation of peroxyxynitrite through a pseudo-second-order post-discharge reaction of H_2O_2 and HNO_2 , *Plasma Sources Sci. Technol.*, 2014, **23**, 15019.
- 40 M. M. Hefny, C. Pattyn, P. Lukes and J. Benedikt, Atmospheric plasma generates oxygen atoms as oxidizing species in aqueous solutions, *J. Phys. D: Appl. Phys.*, 2016, **49**, 404002.
- 41 J. Winter, H. Tresp, M. U. Hammer, S. Iseni, S. Kupsch, A. Schmidt-Bleker, K. Wende, M. Dünbnier, K. Masur, K.-D. Weltmann and S. Reuter, Tracking plasma generated H_2O_2 from gas into liquid phase and revealing its dominant impact on human skin cells, *J. Phys. D: Appl. Phys.*, 2014, **47**, 285401.
- 42 B. H. J. Bielski, D. E. Cabelli, R. L. Arudi and A. B. Ross, Reactivity of HO_2/O_2^- Radicals in Aqueous Solution, *J. Phys. Chem. Ref. Data*, 1985, **14**, 1041–1100.
- 43 D. Madsen, J. Larsen, S. K. Jensen, S. R. Keiding and J. Thøgersen, The Primary Photodynamics of Aqueous Nitrate: Formation of Peroxyxynitrite, *J. Am. Chem. Soc.*, 2003, **125**, 15571–15576.
- 44 A. M. Lietz and M. J. Kushner, Air plasma treatment of liquid covered tissue: long timescale chemistry, *J. Phys. D: Appl. Phys.*, 2016, **49**, 425204.
- 45 P. Lukeš, B. R. Locke and J.-L. Brisset, Aqueous-Phase Chemistry of Electrical Discharge Plasma in Water and in Gas-Liquid Environment, in *Plasma Chemistry and Catalysis in Gases and Liquids*, ed. V. I. Parvulescu, M. Magureanu and P. Lukeš, Wiley-VCH Verlag GmbH & Co. KGaA, 2012, ch. 7.
- 46 J.-L. Brisset and E. Hnatiuc, Peroxyxynitrite: a re-examination of the chemical properties of non-thermal discharges burning in air over aqueous solutions, *Plasma Chem. Plasma Process.*, 2012, **32**, 655–674.
- 47 J. S. Beckman, T. W. Beckman, J. Chen, P. A. Marshall and B. A. Freeman, Apparent hydroxyl radical production by peroxyxynitrite: implications for endothelial injury from nitric oxide and superoxide, *Proc. Natl. Acad. Sci. U. S. A.*, 1990, **87**, 1620–1624.
- 48 S. Goldstein, J. Lind and G. Merényi, Chemistry of peroxyxynitrites as compared to peroxyxynitrates, *Chem. Rev.*, 2005, **105**, 2457–2470.
- 49 M. Naïtali, J.-M. Herry, E. Hnatiuc, G. Kamgang and J.-L. Brisset, Kinetics and bacterial inactivation induced by peroxyxynitrite in electric discharges in air, *Plasma Chem. Plasma Process.*, 2012, **32**, 675–692.
- 50 K. Oehmigen, J. Winter, M. Hähnel, C. Wilke, R. Brandenburg, K. D. Weltmann and T. von Woedtke, Estimation of possible mechanisms of *Escherichia coli* inactivation by plasma treated sodium chloride solution, *Plasma Processes Polym.*, 2011, **8**, 904–913.
- 51 C. A. J. van Gils, S. Hofmann, B. K. H. L. Boekema, R. Brandenburg and P. J. Bruggeman, Mechanisms of bacterial inactivation in the liquid phase induced by a remote RF cold atmospheric pressure plasma jet, *J. Phys. D: Appl. Phys.*, 2013, **46**, 175203.
- 52 F. Girard, V. Badets, S. Blanc, K. Gazeli, L. Marlin, L. Authier, P. Svarnas, N. Sojic, F. Clément and S. Arbault, Formation of reactive nitrogen species including peroxyxynitrite in physiological buffer exposed to cold atmospheric plasma, *RSC Adv.*, 2016, **6**, 78457–78467.
- 53 T. Loegager and K. Sehested, Formation and decay of peroxyxynitrous acid: a pulse radiolysis study, *J. Phys. Chem.*, 1993, **97**, 6664–6669.
- 54 S. Goldstein and G. Czapski, The reaction of NO^\bullet with $\text{O}_2^{\bullet-}$ and HO_2^\bullet : a pulse radiolysis study, *Free Radical Biol. Med.*, 1995, **19**, 505–510.
- 55 H. Ischiropoulos, J. S. Beckman, J. P. Crow, Y. Z. Ye, J. A. Royall and N. W. Kooy, Detection of peroxyxynitrite, *Methods A Companion to Methods Enzymol.*, 1995, **7**, 109–115.
- 56 X. Chen, H. Chen, R. Deng and J. Shen, Pros and cons of current approaches for detecting peroxyxynitrite and their applications, *Biomed. J.*, 2014, **37**, 120–126.
- 57 R. Radi, G. Peluffo, M. N. Alvarez, M. Naviliat and A. Cayota, Unraveling peroxyxynitrite formation in biological systems, *Free Radical Biol. Med.*, 2001, **30**, 463–488.
- 58 A. Sikora, J. Zielonka, M. Lopez, J. Joseph and B. Kalyanaraman, Direct oxidation of boronates by peroxyxynitrite: mechanism and implications in fluorescence imaging of peroxyxynitrite, *Free Radical Biol. Med.*, 2009, **47**, 1401–1407.
- 59 J. Tian, H. Chen, L. Zhuo, Y. Xie, N. Li and B. Tang, A highly selective, cell-permeable fluorescent nanoprobe for ratiometric detection and imaging of peroxyxynitrite in living cells, *Chem. – Eur. J.*, 2011, **17**, 6626–6634.
- 60 B. Kalyanaraman, V. Darley-Usmar, K. J. A. Davies, P. A. Dennery, H. J. Forman, M. B. Grisham, G. E. Mann, K. Moore, L. J. Roberts and H. Ischiropoulos, Measuring reactive oxygen and nitrogen species with fluorescent probes: challenges and limitations, *Free Radical Biol. Med.*, 2012, **52**, 1–6.
- 61 C. C. Winterbourn, The challenges of using fluorescent probes to detect and quantify specific reactive oxygen species in living cells, *Biochim. Biophys. Acta, Gen. Subj.*, 2014, **1840**, 730–738.
- 62 X. Chen, Z. Zhong, Z. Xu, L. Chen and Y. Wang, 2',7'-Dichlorodihydrofluorescein as a fluorescent probe for reactive oxygen species measurement: forty years of application and controversy, *Free Radical Res.*, 2010, **44**, 587–604.
- 63 A. S. Keston and R. Brandt, The fluorometric analysis of ultramicro quantities of hydrogen peroxide, *Anal. Biochem.*, 1965, **11**, 1–5.
- 64 M. Wrona, K. Patel and P. Wardman, Reactivity of 2',7'-dichlorodihydrofluorescein and dihydrorhodamine 123 and their oxidized forms toward carbonate, nitrogen dioxide, and hydroxyl radicals, *Free Radical Biol. Med.*, 2005, **38**, 262–270.
- 65 O. Myhre, J. M. Andersen, H. Aarnes and F. Fonnum, Evaluation of the probes 2',7'-dichlorofluorescein diacetate,

- luminol, and lucigenin as indicators of reactive species formation, *Biochem. Pharmacol.*, 2003, **65**, 1575–1582.
- 66 C. A. Cohn, S. R. Simon and M. A. Schoonen, Comparison of fluorescence-based techniques for the quantification of particle-induced hydroxyl radicals, *Part. Fibre Toxicol.*, 2008, **5**, 1–9.
- 67 H. Possel, H. Noack, W. Augustin, G. Keilhoff and G. Wolf, 2,7-Dihydrodichlorofluorescein diacetate as a fluorescent marker for peroxynitrite formation, *FEBS Lett.*, 1997, **416**, 175–178.
- 68 J. P. Crow, Dichlorodihydrofluorescein and dihydrorhodamine 123 are sensitive indicators of peroxynitrite *in vitro*: implications for intracellular measurement of reactive nitrogen and oxygen species, *Nitric oxide Biol. Chem.*, 1997, **1**, 145–157.
- 69 N. W. Kooy, J. A. Royall and H. Ischiropoulos, Oxidation of 2',7'-dichlorofluorescein by peroxynitrite, *Free Radical Res.*, 1997, **27**, 245–254.
- 70 S. L. Hempel, G. R. Buettner, Y. Q. O'Malley, D. A. Wessels and D. M. Flaherty, Dihydrofluorescein diacetate is superior for detecting intracellular oxidants: comparison with 2',7'-dichlorodihydrofluorescein diacetate, 5-(and 6)-carboxy-2',7'-dichlorodihydrofluorescein diacetate, and dihydrorhodamine 123, *Free Radical Biol. Med.*, 1999, **27**, 146–159.
- 71 M. Janda, Z. Machala, A. Niklová and V. Martišoviř, The streamer-to-spark transition in a transient spark: a dc-driven nanosecond-pulsed discharge in atmospheric air, *Plasma Sources Sci. Technol.*, 2012, **21**, 45006.
- 72 M. Janda, V. Martišoviř, K. Hensel and Z. Machala, Generation of Antimicrobial NO_x by Atmospheric Air Transient Spark Discharge, *Plasma Chem. Plasma Process.*, 2016, **36**, 767–781.
- 73 B. Pongrác, H. H. Kim, M. Janda, V. Martišoviř and Z. Machala, Fast imaging of intermittent electro-spraying of water with positive corona discharge, *J. Phys. D: Appl. Phys.*, 2014, **47**, 315202.
- 74 G. M. Eisenberg, Colorimetric Determination of Hydrogen Peroxide, *Ind. Eng. Chem., Anal. Ed.*, 1943, **15**, 327–328.
- 75 H. Tresp, M. U. Hammer, J. Winter, K.-D. Weltmann and S. Reuter, Quantitative detection of plasma-generated radicals in liquids by electron paramagnetic resonance spectroscopy, *J. Phys. D: Appl. Phys.*, 2013, **46**, 435401.
- 76 K. Setsukinai, Y. Urano, K. Kakinuma, H. J. Majima and T. Nagano, Development of novel fluorescence probes that can reliably detect reactive oxygen species and distinguish specific species, *J. Biol. Chem.*, 2003, **278**, 3170–3175.
- 77 B. Tarabová, P. Lukeř, M. Janda, K. Hensel, L. Šikurová and Z. Machala, Specificity of detection methods of nitrites and ozone in aqueous solutions activated by air plasma, *Plasma Processes Polym.*, 2018, e1800030.
- 78 Z. Machala, B. Tarabová, D. Sersenová, M. Janda and K. Hensel, Chemical and antibacterial effects of plasma activated water: correlation with gaseous and aqueous reactive oxygen and nitrogen species, plasma sources and air flow conditions, *J. Phys. D: Appl. Phys.*, 2018, **52**, 034002.
- 79 H. Tong, A. M. Arangio, P. S. J. Lakey, T. Berkemeier, F. Liu, C. J. Kampf, W. H. Brune, U. Pöschl and M. Shiraiwa, Hydroxyl radicals from secondary organic aerosol decomposition in water, *Atmos. Chem. Phys.*, 2016, **16**, 1761–1771.
- 80 C. Walling and T. Weil, The Ferric Ion Catalyzed Decomposition of Hydrogen Peroxide in Perchloric Acid Solution, *Int. J. Chem. Kinet.*, 1974, **VI**, 507–516.
- 81 J. De Laat and H. Gallard, Catalytic decomposition of hydrogen peroxide by Fe(III) in homogeneous aqueous solution: mechanism and kinetic modeling, *Environ. Sci. Technol.*, 1999, **33**, 2726–2732.
- 82 P. Lukes, H. Tresp, S. Reuter, E. Dolezalova, M. Clupek and T. von Woedtke, in *14th International Symposium on High Pressure Low Temperature Plasma Chemistry (HAKONE 2014)*, ed. R. Brandenburg and L. Stollenwerk, INP Greifswald, IfP Greifswald, 2014.
- 83 J. Glebska and W. H. Koppenol, Peroxynitrite-mediated oxidation of dichlorodihydrofluorescein and dihydrorhodamine, *Free Radical Biol. Med.*, 2003, **35**, 676–682.
- 84 H. Masumoto and H. Sies, The reaction of ebselen with peroxynitrite, *Chem. Res. Toxicol.*, 1996, **9**, 1057–1062.
- 85 H. Masumoto, R. Kissner, W. H. Koppenol and H. Sies, Kinetic study of the reaction of glutathione peroxidase with peroxynitrite, *FEBS Lett.*, 1996, **398**, 179–182.
- 86 A. Mouithys-Mickalad Mareque, J. M. Faez, L. Chistiaens, S. Kohnen, C. Deby, M. Hoebeke, M. Lamy and G. Deby-Dupont, *In vitro* evaluation of glutathione peroxidase (GPx)-like activity and antioxidant properties of some Ebselen analogues, *Redox Rep.*, 2004, **9**, 81–87.
- 87 B. K. Sarma and G. Mughesh, Antioxidant activity of the anti-inflammatory compound ebselen: a reversible cyclization pathway *via* selenenic and seleninic acid intermediates, *Chem. – Eur. J.*, 2008, **14**, 10603–10614.
- 88 R. Zhao and A. Holmgren, A novel antioxidant mechanism of ebselen involving ebselen diselenide, a substrate of mammalian thioredoxin and thioredoxin reductase, *J. Biol. Chem.*, 2002, **277**, 39456–39462.
- 89 O. I. Aruoma, B. Halliwell, B. M. Hoey and J. Butler, The antioxidant action of taurine, hypotaurine and their metabolic precursors, *Biochem. J.*, 1988, **256**, 251–255.
- 90 M. W. S. Oliveira, J. B. Minotto, M. R. de Oliveira, A. Zanotto-Filho, G. A. Behr, R. F. Rocha, J. C. F. Moreira and F. Klamt, Scavenging and antioxidant potential of physiological taurine concentrations against different reactive oxygen/nitrogen species, *Pharmacol. Rep.*, 2010, **62**, 185–193.
- 91 M. Fontana, L. Pecci, S. Duprè and D. Cavallini, Antioxidant Properties of Sulfinates: Protective Effect of Hypotaurine on Peroxynitrite-Dependent Damage, *Neurochem. Res.*, 2004, **29**, 111–116.
- 92 D. Dobrynin, K. Arjunan, A. Fridman, G. Friedman and A. M. Clyne, Direct and controllable nitric oxide delivery into biological media and living cells by a pin-to-hole spark discharge (PHD) plasma, *J. Phys. D: Appl. Phys.*, 2011, **44**, 075201.
- 93 V. Jirásek and P. Lukeř, in *Book of Extended Abstracts, International Symposium on Plasma Chemistry (ISPC 23)*, Montréal (Canada), 2017, pp. 3–4.